



Vibratory Coupling Between Strings and Soundbox in Bowed Instruments

Francesco Sorge¹

Received: 16 November 2022 / Revised: 24 March 2023 / Accepted: 25 April 2023 / Published online: 18 May 2023
© Krishtel eMaging Solutions Private Limited 2023

Abstract

This paper deals with the string instruments of the violin family and addresses, in particular, the vibration coupling between the four strings and the soundbox in the low-frequency range. The analysis is applicable to any type of multi-chord excitation by the bow though it is here developed for the bichord case. Proper dynamical models of the single parts constituting the complete system are presented and an accurate kinematical–dynamical study of the bridge interfacing between the strings and the top plate of the soundbox permits to relate the forces and the displacements on the exciting and the sound-emitting components of the instrument. The characteristic equation is formulated and the coupled frequency spectrum is obtained based on realistic hypotheses about the distinctive mechanical properties of the single instrument parts. Then, a proper model is proposed to describe the nonlinear stick–slip contact between the bow and the strings and the numerical integration of the motion equations is performed by a modal decomposition approach. In parallel, applying the approximate hypothesis of periodic Helmholtz motions of the strings, simple analytical solutions for the soundbox vibrations are carried out and compared with the numerical response. The latter shows small aperiodic fluctuations of the amplitude and slow phase shifts in comparison with the periodic analytical solutions, which may, however, be accepted as an approximate description of the instrument behaviour.

Keywords Bowed string instrument · Chord-box coupling · Stick–slip · Modal approach · Numerical solution · Analytical approximation

Introduction

The first theoretical studies on the vibratory performances of the bowed string instruments date back to the early approaches of Helmholtz and Raman [1, 2], which give precise analytical descriptions of the characteristic wave propagation along the violin strings. Yet, scientific interest began to grow greatly only from the middle of the twentieth century up until today, looking into the various specific aspects of the string–soundbox dynamics and the influence of the material characteristics. Among plenty of papers of the theoretical and experimental kinds, we here cite a few examples of a certain significance.

References [3, 4] outline the physics of the violin strings and the acoustic characteristics of the vibrating plates of the soundbox, while extensive and detailed descriptions of the mechanics of the bowed string instruments are reported in the books [5, 6], together with a large collection of experimental data. As well known, the excitation of the violin vibration arises from the stick–slip motion of the string relative to the dragging bow, which may be significantly affected by local factors, such as the temperature, the rosin spreading on the bow to increase friction and the possible unsteadiness of the bow motion. Researches on the bow–string contact behaviour are reported in references [7–11], showing the various force–speed characteristic curves depending on the working conditions. The state of the art on research on the various aspects of violin sound production is fixed in [12, 13]. Other studies concern the different responses of the string instruments depending on the materials used for their manufacture, the wood varnishing, the plate thickness, and so on [14, 15]. Besides, the motion of a cello bridge in the low-frequency range is inspected experimentally [16] and

Francesco Sorge retired since 2018.

✉ Francesco Sorge
francesco.sorge@you.unipa.it

¹ Department of Engineering, University of Palermo,
90128 Palermo, Italy

the response in the high-frequency range is theoretically analysed in reference [17].

The theoretical description of the kinematic–dynamic interfacing between the excited strings, which stimulate the system vibrations without emitting sound, and the harmonic box, which has the task of generating the sound and giving the proper tone colour, is quite hard due to the involvement of many complex aspects associated with the progressing and reflecting waves along the strings, their dissipation, the definition of the nonlinear stick–slip dragging force of the bow, the vibration coupling between the bridge and the soundbox and several other secondary effects. The present analysis moves from the intent of outlining an overall modal description of the instrument behaviour, looking first for the natural frequencies of the whole interconnected system and then calculating the time response by eigenfunction expansion. The novelty of the approach stays mainly in the wholeness of the outlook, which is not limited to single aspects of the instrument behaviour, as frequent in many other studies due to the great complexity of the bow instrument properties.

At the same time, the following dynamical model will necessarily introduce some simplifying hypotheses as, otherwise, a very accurate and comprehensive analysis would be extremely hard, if not impossible.

Going after a previous paper [18], the author focuses in particular on the string–soundbox coupling in the low-frequency range, that is the range of the signature modes, carrying out a numerical–analytical modal approach in parallel, to identify the coupling effects on the dynamical response of the instrument and work out possible approximate models of the sound production. In practice, the results give a sort of "skeleton" solution to which the high-frequency components should after be attached.

The analysis introduces suitable functional relations between the forces and the displacements at the string–bridge contact and those at the bridge feet, for symmetric, antisymmetric and general modes of the soundbox. The characteristic equation of the coupled system is formulated and, assuming realistic values for the soundbox's frequencies, the coupled frequency spectrum is identified. A proper theoretical model of the bow–string stick–slip contact is formulated, where the adhesion force required during the stick phase and the bow–string sliding speed during the slip phase are continuously monitored to pass from one to the other phase automatically during the calculation. After solving the motion equations numerically in the time domain, the results are compared with the approximate analytical solutions obtainable assuming the ideal Helmholtz motion as the string exciting motion.

The present analysis considers a bichord excitation of the bow with two open or fingered strings but can be extended to other multichord cases.

Natural Modes

Mathematical Modelling of the String Sub-systems

Consider a violin like that in Fig. 1 and assume the combination nut–chinrest–violinist as a fixed rigid reference for simplicity. The four open strings, $G3$, $D4$, $A4$ and $E5$, have frequencies 196 Hz, 294 Hz, 440 Hz and 659 Hz, respectively, and each of them may be referred separately to its own fixed frame $O_S x_S y_S z_S$, with the origin O_S on the nut, the x_S -axis along the straight string position in non-vibrating conditions and the $x_S y_S$ plane tangent to the bridge top as in Fig. 1. Here and in the following, the subscript S indicates one generic string among G ($G3$), D ($D4$), A ($A4$) and E ($E5$). It is supposed that the extremes of the violin strings on the bridge are placed, on the upper bridge profile, symmetrically and equally distributed along a circumference whose centre C is located under the mid-point P_M of the bridge basis $P_B P_T$ on the top plate of the soundbox (see Fig. 2). Here P_B and P_T are the points where the resultant reaction forces of the soundbox

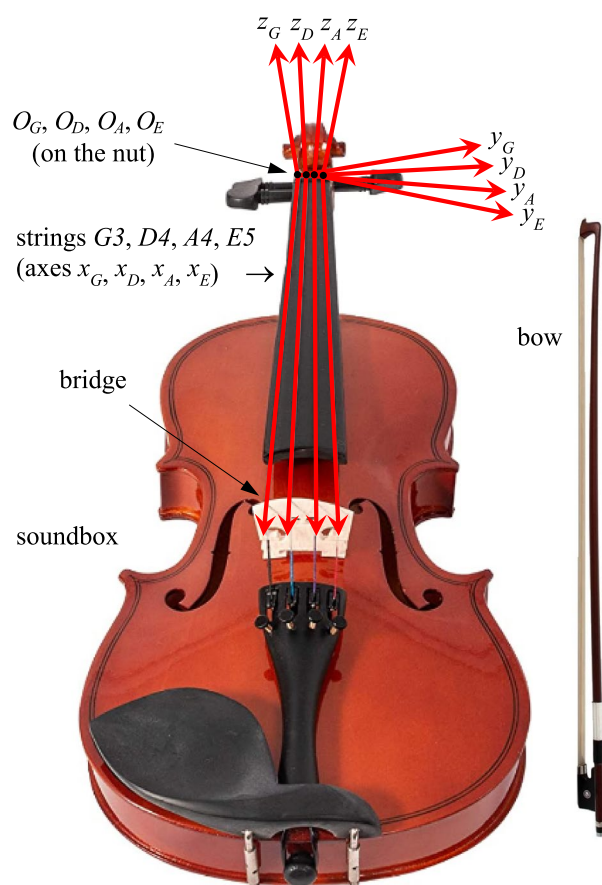
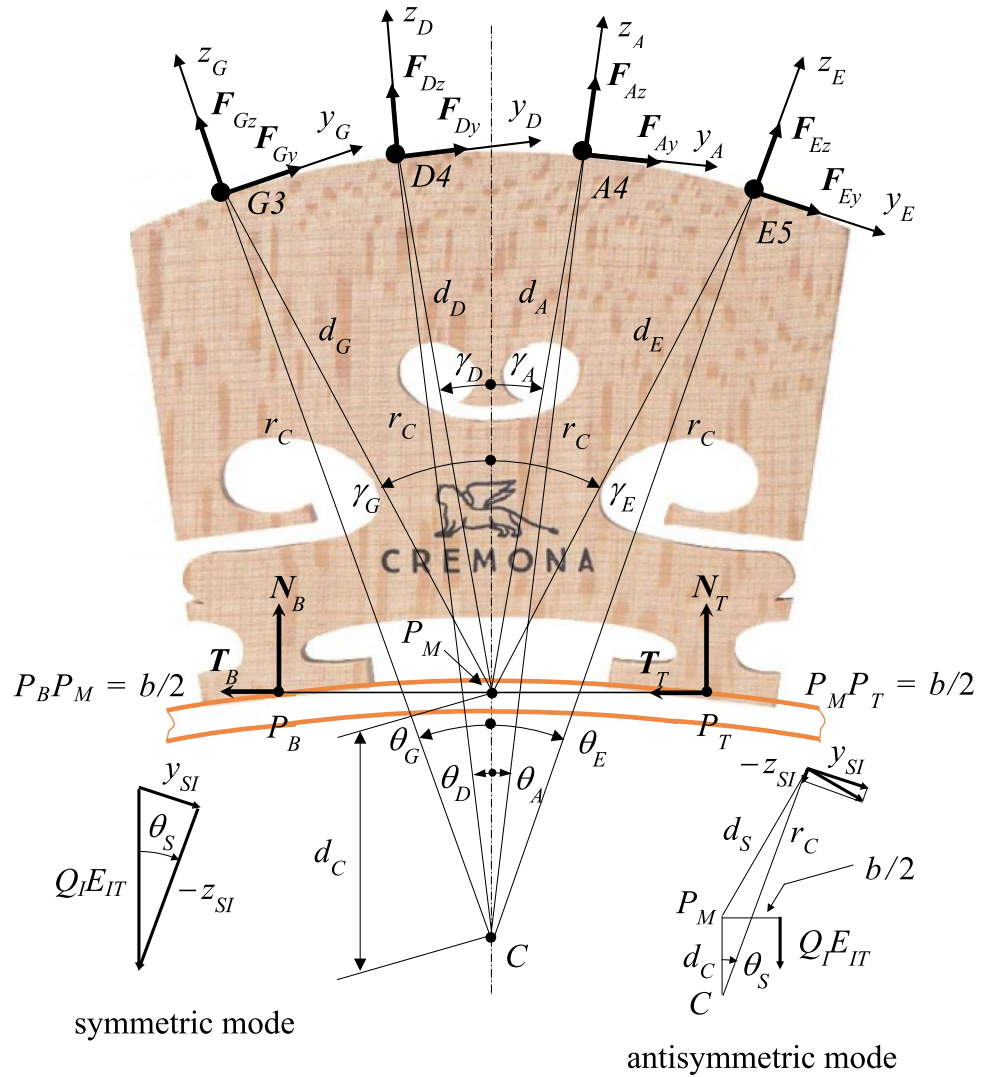


Fig. 1 Front view of a violin and reference frames on the four open strings

Fig. 2 Bridge geometry. Forces and displacements of strings and soundbox. Case of free vibrations. $d_G=d_E, d_D=d_A, \gamma_G=\gamma_E, \gamma_D=\gamma_A, \theta_G=\theta_E, \theta_D=\theta_A$



may be considered applied, on the bass and treble sides, respectively.

The distances d_S of the string ends from the point P_M are related to the bridge top radius r_C , to the distance d_C of P_M from C and to the angles θ_S by the Carnot formula (see Fig. 2)

$$d_S = \sqrt{d_C^2 + r_C^2 - 2d_C r_C \cos \theta_S}, \tag{1}$$

while the angles γ_S formed with the symmetry axis of the bridge are obtainable by the relation (see Fig. 2)

$$\tan (\gamma_S - \theta_S) = \frac{d_C \sin \theta_S}{r_C - d_C \cos \theta_S}. \tag{2}$$

The displacement of the points of each string along the y_S and z_S transverse directions may be expanded in two corresponding series of sinusoidal eigenfunctions,

$e_{S_{yi}}(x_S) = a_{S_{yi}} \sin(\omega_i x_S / v_{wS})$ and $e_{S_{zi}}(x_S) = a_{S_{zi}} \sin(\omega_i x_S / v_{wS})$, multiplied by generalized coordinates $q_{S_{yi}}(t)$ and $q_{S_{zi}}(t)$, that is $y_S(x, t) = \sum_i q_{S_{yi}}(t) e_{S_{yi}}(x_S)$ and $z_S(x, t) = \sum_i q_{S_{zi}}(t) e_{S_{zi}}(x_S)$. Here, the subscript i refers to the natural modes of the total system string + soundbox, the ω_i are the corresponding natural frequencies, $v_{wS} = \sqrt{T_S / (\mu_S S_S)}$ is the wave propagation speed, where T_S is the string tensioning, μ_S and S_S are the mass density and the cross-section area of the string, which are all different for each string. Thus, since one has $f_S = \omega_S / (2\pi) = v_{wS} / (2l_S) = \sqrt{T_S / (\mu_S S_S)} / (2l_S)$ for the fundamental frequency of an isolated string between fixed extremes, where l_S is the string length, the tuning is obtainable by adjusting the only tension T_S , as well known. The eigenfunctions $e_{S_{yi}}(x_S)$ and $e_{S_{zi}}(x_S)$ have the same form as in the canonical case of a string with fixed ends because

the linear non-dissipative operators of the two problems are the same, $(\partial^2 y_s / \partial t^2) / (\partial^2 y_s / \partial x_s^2) = (\partial^2 z_s / \partial t^2) / (\partial^2 z_s / \partial x_s^2) = v_{ws}^2$ (d'Alembert equation). Nevertheless, they are not to be considered orthogonal to each other now, nor are the frequencies in rigorous arithmetical progression, because the boundary conditions differ from the canonical case since the string extremes on the bridge side vibrate together with the bridge and the soundbox.

Observe that $q_{si} = q_{si,max} \sin \omega_i t$ for the natural modes.

Mathematical Modelling of the Soundbox Sub-system

The violin strings could not emit a vigorous and harmonious sound by themselves but need the dynamic contribution of the soundbox. Considering the soundbox as an

evaluating the bandwidths of the singular modes and then the damping factors Z_l . The present analysis is just limited to the lower modes ($< \sim 1500$ Hz), which are clearly identifiable in the frequency response. As well known, the high-frequency range covers the so-called "bridge hill" region, where a diffused overlap of bandwidths occurs, the modal approach would require great skill to get realistic results, or other methods should be applied (e.g. see [17]). The whole frequency spectrum of the instruments should be obtained by joining the two frequency ranges.

Figure 2 shows the forces applied to the bridge by the strings and the soundbox top plate. As the bridge's frequencies are considerably higher than the examined range, the bridge may be presumed rigid and its mass may be neglected (see also [16]). Hence, disregarding the possible moment of $T_T + T_B$ with respect to P_M , which is certainly negligible, and using Eqs. (1–2), the calculation of the normal reaction forces at the bridge feet by the equilibrium conditions is quite straightforward:

$$\begin{aligned}
 N_T &= \frac{1}{2} \left[\sum_{S=G,D,A,E} (F_{Sy} \sin \theta_S - F_{Sz} \cos \theta_S) + \frac{2(r_C - d_C \cos \theta_S)}{b} F_{Sy} - \frac{2d_C}{b} F_{Sz} \sin \theta_S \right], \\
 N_B &= \frac{1}{2} \left[\sum_{S=G,D,A,E} (F_{Sy} \sin \theta_S - F_{Sz} \cos \theta_S) - \frac{2(r_C - d_C \cos \theta_S)}{b} F_{Sy} + \frac{2d_C}{b} F_{Sz} \sin \theta_S \right].
 \end{aligned}
 \tag{3}$$

isolated system and, using capital letters for clearness to denote the quantities involved in its vibratory motion, introduce the natural frequencies Ω_l , the two-dimensional eigenfunctions E_l and the modal coordinates Q_l , where the subscripts l refer to the single characterizing modes of the soundbox alone. The domain of the eigenfunctions E_l is the whole vibrating surface of the soundbox, including the top plate, the back plate and the ribs, so an approach by partial differential equations would result prohibitive. Nevertheless, by partitioning this surface into a great number of very small elements, the problem becomes of the finite-difference or finite element types, with a very large but finite number of degrees of freedom. Hence, the conventional approach to linear discrete systems should ensure the orthogonality of the vibrating modes and allow the mode separation and the normalization of the discretized eigenfunctions. In practice, it is here presumed that the quantities Ω_l and E_l are obtainable by experimental tests, e.g. by holographic interferometry or impulse hammer and accelerometers or laser Doppler vibrometry. On the other hand, other experiments should also permit

Four constant forces $F_{Sz0} < 0$, induced by the constant tensioning of the strings and converging in C along SC , are included in the four forces F_{Sz} , but they yield only invariant deflections of the string and the soundbox and are then irrelevant for the present analysis of the vibratory motion. Thus, they may be ignored in the calculation of the F_{Sz} in all vibration studies.

The concentrated forces on the soundbox surface, N_T and N_B downward directed, may be dealt with using two-dimensional Dirac distributions, $\delta(X - X_*, Y - Y_*)$, where X and Y are the coordinates on this surface and X_* and Y_* refer to the force application point. Applying the usual modal separation technique to the soundbox motions, even though within a discretized model, i.e. multiplying the discretized partial differential equation of the soundbox vibration by each single eigenfunction $E_l(X, Y)$ and integrating, i.e. summing to all elements, these forces turn out to be multiplied by $E_l(X_{PT}, Y_{PT}) = E_{lT}$ and $E_l(X_{PB}, Y_{PB}) = E_{lB}$ for each mode l , and moreover, $E_{lB} = E_{lT}$ and $E_{lB} = -E_{lT}$ for the symmetric and antisymmetric mode shapes of the top plate, respectively. Therefore, using P_T as a unique reference point, the overall effect for each mode l is

$$\begin{aligned}
 & E_{IT}N_T + E_{IB}N_B \\
 &= E_{IT}(N_T + N_B) \\
 &= E_{IT} \sum_{S=G,D,A,E} (F_{Sy} \sin \theta_S - F_{Sz} \cos \theta_S) \quad (\text{for symmetric modes}) \\
 & E_{IT}N_T + E_{IB}N_B = E_{IT}(N_T - N_B) \\
 &= E_{IT} \sum_{S=G,D,A,E} \left[\frac{2(r_C - d_C \cos \theta_S)}{b} F_{Sy} - \frac{2d_C}{b} F_{Sz} \sin \theta_S \right] \\
 & (\text{for antisymmetric modes}) \text{whence } E_{IT}N_T + E_{IB}N_B \\
 &= E_{IT} \sum_{S=G,D,A,E} (c_{Sy}F_{Sy} - c_{Sz}F_{Sz})
 \end{aligned} \tag{4}$$

where the following force coefficients, c_{sy} and c_{sz} , have been introduced

$$\begin{aligned}
 c_{Sy} &= \sin \theta_S \quad c_{Sz} = \cos \theta_S \quad (\text{for the symmetric modes}) \\
 c_{Sy} &= \frac{2(r_C - d_C \cos \theta_S)}{b} \quad c_{Sz} = \frac{2d_C}{b} \sin \theta_S \\
 & (\text{for the antisymmetric modes}).
 \end{aligned} \tag{5}$$

On the other hand, the soundbox vibratory displacements, even though quite small if compared with the strings, imply vibration components of the strings on both, the $x_S y_S$ and the $x_S z_S$ planes. The normal displacements of points P_T and P_B towards the box inside may be expressed by the modal sums $\sum_I Q_I E_{IT}$ and $\sum_I Q_I E_{IB}$, where $E_{IB} = \pm E_{IT}$ for the symmetric and antisymmetric modes of the top plate. Decomposing also the y and z displacements of the string ends, $y_S(l_S, t)$ and $z_S(l_S, t)$, into sums of modal components, $y_S(l_S, t) = \sum_I y_{SI}(l_S, t)$ and $z_S(l_S, t) = \sum_I z_{SI}(l_S, t)$, these components may be related to the corresponding modal components of the soundbox by the following kinematical equations

$$\begin{aligned}
 y_{SI} &= Q_I E_{IT} \sin \theta_S \quad z_{SI} = -Q_I E_{IT} \cos \theta_S \quad (\text{symmetric modes}) \\
 y_{SI} &= Q_I E_{IT} \frac{2(r_C - d_C \cos \theta_S)}{b} \quad z_{SI} = -Q_I E_{IT} \frac{2d_C}{b} \sin \theta_S \\
 & (\text{antisymmetric modes})
 \end{aligned} \tag{6}$$

according to the vectorial diagrams in Fig. 2.

Hence, one may write $y_{SI} = c_{Sy} Q_I E_{IT}$ and $z_{SI} = -c_{Sz} Q_I E_{IT}$, where the displacement coefficients c_{Sy} and c_{Sz} are given by Eq. (5) and are equal to the previous force coefficients, in perfect accordance with the virtual work principle. Actually, multiplying the last equality of Eq. (4) by Q_I and accounting for Eq. (6) one observes that the total work of the forces applied to the bridge is zero for each mode I and then for the sum of all modes.

It must be clarified that the introduction of the sound post and the bass bar in the inside of the harmonic box

modifies its symmetry characteristic in comparison with the preliminary artefact with no additional elements, whence each mode shape turns out to be some complicated combination of symmetric and antisymmetric shapes. Therefore, to address this problem, the above coefficients, c_{Sy} and c_{Sz} , may be combined approximately by proper weighting coefficients, somehow guided by the results from the experimentation. In practice, indicating with p_s and p_a the values of any of these parameters, c_{Sy} and c_{Sz} , for the symmetric and antisymmetric deformation, respectively, we may set $p_I = p_{sI} w_{sI} + p_{aI} (1 - w_{sI})$ (with $0 < w_{sI} < 1$), where w_{sI} is the "weight" of the symmetric shape in the specific mode I . Therefore, a set of pairs c_{SyI} and c_{SzI} applies to the various soundbox modes I .

Assume normalized eigenfunctions of the soundbox, so that $\int_0^{S_p} \mu_p h_p E_R E_S dX dY = \delta_{RS}$, where the integrals must be understood as summations in the hypothesis of discretization of the domain, μ_p , h_p and S_p are the mass density, the thickness and the whole surface area of the vibrating soundbox and δ_{RS} is the Kronecker delta. Incidentally, observe that the order of magnitude of the products $E_R E_S$ is the reciprocal of that of the soundbox mass $\mu_p h_p S_p$, according to the above normalization condition.

The usual modal separation technique yields the motion equations of the soundbox sub-system when excited by the downward forces N_T and N_B ,

$$\frac{d^2 Q_I}{dt^2} + \Omega_I^2 Q_I = E_{IT} \sum_{S=G,D,A,E} (c_{SyI} F_{Sy} - c_{SzI} F_{Sz}) \quad I = 1, 2, \dots, \tag{7}$$

where Eq. (4) is used and the dissipation is ignored as we are searching for the natural modes.

Frequency Spectrum

The search for the natural modes implies replacing $F_{Sy} = -T_S \times \sum_i q_{Syi} (de_{Syi}/dx)_{x=l_S}$ and $F_{Sz} = -T_S \times \sum_i q_{Szi} (de_{Szi}/dx)_{x=l_S}$ into Eq. (7), for $S = G, D, A$ and B , and solving for the Q_I .

$$\begin{aligned}
 Q_I &= -E_{IT} \sum_{S=G,D,A,E} T_S \sum_i (c_{SyI} a_{Syi} q_{Syi, \max} - c_{SzI} a_{Szi} q_{Szi, \max}) \\
 & \left(\frac{\omega_i}{v_{wS}} \right) \cos \left(\frac{\omega_i l_S}{v_{wS}} \right) \frac{\sin(\omega_i t)}{\Omega_I^2 - \omega_i^2} \quad I = 1, 2, \dots
 \end{aligned} \tag{8}$$

Hence, using Eq. (6) for the displacements of the generic string S' , one has $y_{S'}(t) = \sum_I y_{SI}(t) = \sum_I c_{SyI} Q_I(t) E_{IT}$, $z_{S'}(t) = \sum_I z_{SI}(t) = -\sum_I c_{SzI} Q_I(t) E_{IT}$ and then, considering the equality $T_S = \mu_S S_S v_{wS}^2$, using Eq. (8) and setting $\sigma_{Si} = \omega_i l_S / v_{wS}$ and $\Sigma_{SI} = \Omega_I l_S / v_{wS}$ for brevity, gets

$$\begin{aligned}
 \sum_i a_{S'yi} \sin\left(\frac{\omega_i l_{S'}}{v_{wS'}}\right) q_{S'yi, \max.} \sin(\omega_i t) &= \sum_i a_{S'yi} \sin \sigma_{S'i} q_{S'yi, \max.} \sin \omega_i t \\
 &= \sum_i c_{S'yi} E_{IT}^2 \sum_{S=G,D,A,E} m_S \sum_i (c_{S'yi} a_{S'yi} q_{S'yi, \max.} - c_{S'zi} a_{S'zi} q_{S'zi, \max.}) \sin \sigma_{S'i} \sin \omega_i t \sum_i \frac{\sigma_{S'i} \cot \sigma_{S'i}}{\sigma_{S'i}^2 - \Sigma_{S'i}^2} \quad (\text{for } S' = G, D, A, E), \\
 - \sum_i a_{S'zi} \sin\left(\frac{\omega_i l_{S'}}{v_{wS'}}\right) q_{S'zi, \max.} \sin(\omega_i t) &= - \sum_i a_{S'zi} \sin \sigma_{S'i} q_{S'zi, \max.} \sin \omega_i t \\
 &= \sum_i c_{S'zi} E_{IT}^2 \sum_{S=G,D,A,E} m_S \sum_i (c_{S'yi} a_{S'yi} q_{S'yi, \max.} - c_{S'zi} a_{S'zi} q_{S'zi, \max.}) \sin \sigma_{S'i} \sin \omega_i t \sum_i \frac{\sigma_{S'i} \cot \sigma_{S'i}}{\sigma_{S'i}^2 - \Sigma_{S'i}^2} \quad (\text{for } S' = G, D, A, E),
 \end{aligned} \tag{9}$$

where m_S is the mass of the string S .

Since Eq. (9) must hold instant by instant, the summation concerning i and the time functions $\sin(\omega_i t)$ may be dropped, obtaining the characteristic equations in the form:

$$\begin{aligned}
 \sum_{S=G,D,A,E} m_S \sum_i c_{S'yi} E_{IT}^2 [c_{S'yi} (a_{S'yi} \sin \sigma_{S'i} q_{S'yi, \max.}) - c_{S'zi} (a_{S'zi} \sin \sigma_{S'i} q_{S'zi, \max.})] \frac{\sigma_{S'i} \cot \sigma_{S'i}}{\sigma_{S'i}^2 - \Sigma_{S'i}^2} \\
 = (a_{S'yi} \sin \sigma_{S'i} q_{S'yi, \max.}) \quad (\text{for } S' = G, D, A, E) \\
 \sum_{S=G,D,A,E} m_S \sum_i c_{S'zi} E_{IT}^2 [c_{S'yi} (a_{S'yi} \sin \sigma_{S'i} q_{S'yi, \max.}) - c_{S'zi} (a_{S'zi} \sin \sigma_{S'i} q_{S'zi, \max.})] \frac{\sigma_{S'i} \cot \sigma_{S'i}}{\sigma_{S'i}^2 - \Sigma_{S'i}^2} = \\
 = -(a_{S'zi} \sin \sigma_{S'i} q_{S'zi, \max.}) \quad (\text{for } S' = G, D, A, E).
 \end{aligned} \tag{10}$$

Equation (10) forms a linear algebraic system of 8 equations in 8 unknowns (inside round brackets), i.e. the 4 unknowns $(a_{S'yi} \sin \sigma_{S'i} q_{S'yi, \max.})$, plus the 4 unknowns $-(a_{S'zi} \sin \sigma_{S'i} q_{S'zi, \max.})$. This system is homogeneous and may be written in the matrix form $[A - I_8] \times \{\xi\}^T = 0$, where the

coefficients of A are the factors of the 8 unknowns on the left sides of Eq. (10), I_8 is the 8×8 identity matrix and ξ is the vector of the 8 unknowns. Hence, the characteristic equation is $\det [A - I_8] = 0$.

Since the order of magnitude of E_i^2 is that of the reciprocal of the vibrating mass of the soundbox, which is much greater than the string mass m_S , one has $m_S E_i^2 < 1$ and it is easy to deduce from Eq. (10) that the coupled frequencies ω_i

Fig. 3 Diagram of the characteristic determinant D_c vs the frequency ratio f/f_A for the case of open strings with lengths 325 mm (tones $G3, D4, A4, E5$). The circled intersection points with the abscissa axis give the natural frequencies of the coupled system, strings + soundbox. The dotted points give the ideal natural frequencies of the separated components of the instrument

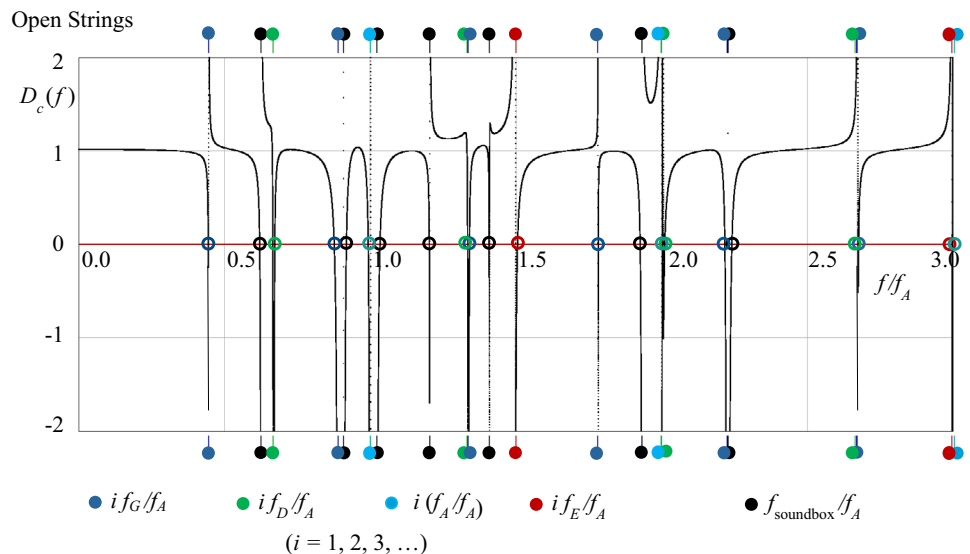
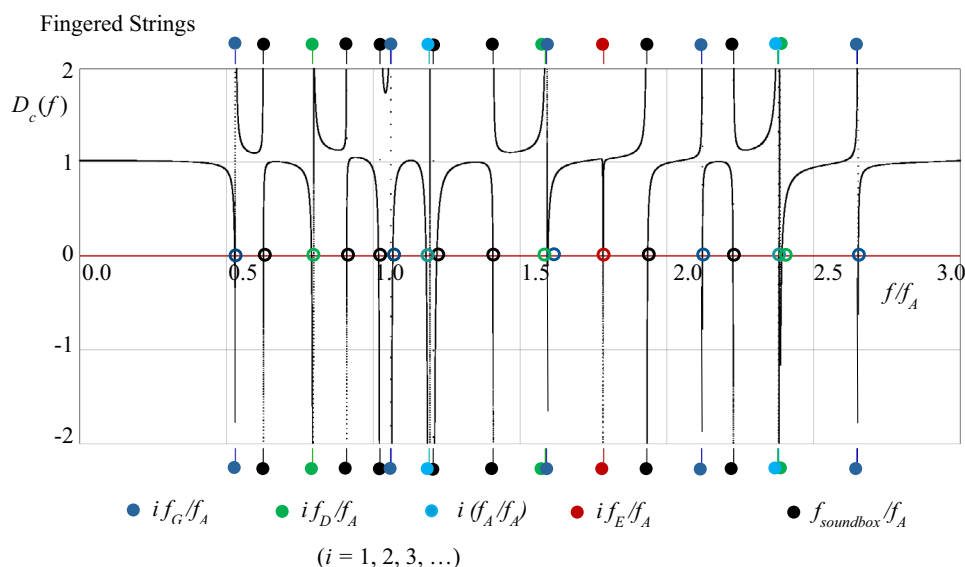


Fig. 4 Diagram of the characteristic determinant D_c vs the frequency ratio f/f_A for the case of fingered strings with lengths 273 mm (tones A#3, F4, C5, G5). The circled intersection points with the abscissa axis give the natural frequencies of the coupled system, strings + soundbox. The dotted points give the ideal natural frequencies of the separated components of the instrument



turn out to be very close to the uncoupled ones, that is, either to $\omega_i \cong i\pi v_{ws}/l_S$ when $\sin(\omega_i l_S/v_{ws}) \cong 0$, for $S = G, D, A$ and E , or to Ω_I , when $\omega_i \cong \Omega_I$. The sequence Ω_I , the eigenfunctions E_I and the coefficients c_{SyI} and c_{SzI} are chosen in the following calculation using verisimilar soundbox properties and realistic values of the weighting coefficients w_{sI} . Once fixing the frequencies Ω_I and all the other parameters, the exact values of the natural frequencies ω_i of the full system may be calculated numerically as roots of the equation $\det [A - I_8] = 0$. It is remarkable that some Ω_I are well separated from the angular frequencies of the strings with fixed–fixed ends, so that the soundbox is feebly excited, whereas some are close to the string frequencies so that the soundbox is resonant and a vigorous sound level is emitted to the surrounding environment.

Figure 3 refers to the open string case and shows the diagram of the characteristic determinant $D_c(f) = \det [A - I_8]$ vs. the dimensionless frequency f/f_A , where the frequency f_A of string A4 was chosen as a reference frequency. The asymptotes for $\sigma_{Si} \cong i\pi$ are clearly observable and indicate the divergence of the function $\cot \sigma_{Si}$, i. e. the very closeness of this series of natural frequencies to that of the single strings S when they are fixed at their extremes. Notice that, since the fundamental frequencies of the four chords have ratios very close to 1.5, each to the next from the treble to the bass sides, some coincidence of the higher harmonics appears for them. Besides, other asymptotes very close to the abscissae f_{soundbox}/f_A , indicate resonant frequencies very close to those of the soundbox.

Figure 4 shows the case of four fingered strings with a shorter length, equal for all of them, so to obtain the four tones A#3, F4, C5, and G5. The frequency scale is the same as in Fig. 3 and a rightward shift of the chord's natural frequencies may be observed.

Summing up, the natural frequencies of the coupled system, strings + soundbox, are very close to those of the single separate components. Nonetheless, the numerical integration of the motion equations for the bowed string case shows some small deviations from the analytical results obtainable by ascribing the "conventional" Helmholtz motion to the string, as will be illustrated in the following.

Vibrations Induced by the Bow

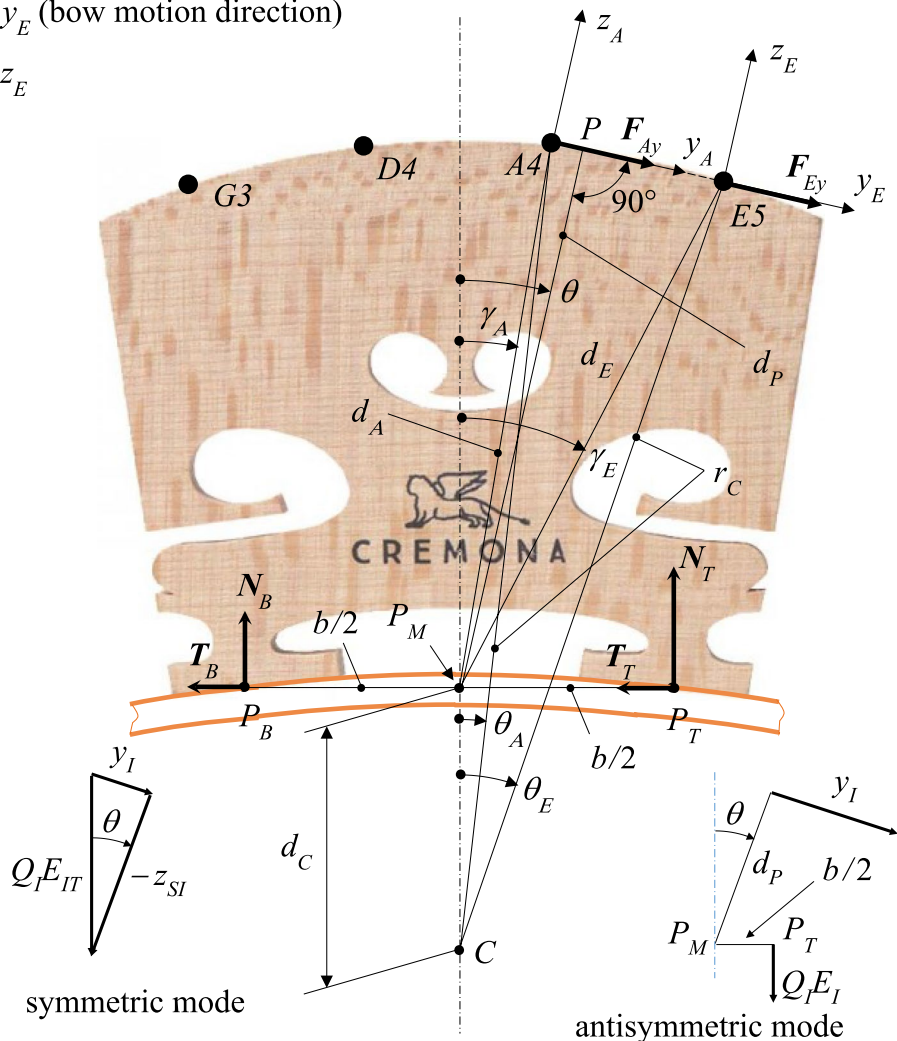
The time solutions for the vibrations excited by the bow may be obtained by the use of solvers of the Euler–Cauchy type, considering a finite but sufficiently large number n of modes. This procedure considers the complete equations of motion, takes care of handling the transfer of forces and displacements correctly at the bridge interface between strings and soundbox, introduces the dissipation terms and formulates the non-linear stick–slip forces of contact between the bow and the single strings using realistic models.

It will be assumed that the bow exerts its drag force only on the third and fourth strings (bichord A4 and E5) and that this force is variably shared between the two strings although the normal bow force applied by the violinist is kept constant, as well as the bow velocity: sure enough, the stick and slip phases alternate differently for the two strings in general. Moreover, according to Fig. 5, it is supposed that the direction of the bow motion is parallel to the straight line joining the endpoints on the bridge of the two strings, A4 and E5, and this straight line will be assumed as the common direction of the y -axes of the two strings. As the prevailing forces at the bridge interface are those produced by the bow drag, the components along z will be neglected, as well as the forces exerted by the other two strings, G3 and D4, though admitting that some small level of vibrations may be transmitted by the soundbox to them.

Fig. 5 Bridge geometry. Forces and displacements of string and soundbox. Case of bow-induced vibrations on strings A4 and E5

$$y_A \equiv y_E \text{ (bow motion direction)}$$

$$z_A \parallel z_E$$



Due to the different geometry of the bowed string case described in Fig. 5 in comparison with Fig. 2, the correlation between forces and displacements at the bridge top and the bridge feet is now different. The distances d_S of the string endpoints from P_M and the angles γ_S are given by Eqs. (1–2), whereas the distance d_P of P_M from the straight-line through the two string endpoints A4 and E5 (common y -axes direction), is given by

$$d_P = d_A \cos(\theta - \gamma_A) = d_E \cos(\theta - \gamma_E), \tag{11}$$

where θ is the angle formed by the z direction with the symmetry axis of the bridge (see Fig. 5). Hence, using Eq. (11), it is possible to calculate the angle θ first

$$\tan \theta = \frac{d_A \cos \gamma_A - d_E \cos \gamma_E}{d_E \sin \gamma_E - d_A \sin \gamma_A} \tag{12}$$

and then d_P .

The bridge equilibrium equations become now, for the bowed case,

$$N_T = \frac{1}{2} \left[(F_{Ay} + F_{Ey}) \left(\sin \theta + \frac{2d_P}{b} \right) + \sum_{S=A,E} \left(F_{Sn} \cos \theta_S + \frac{2d_C}{b} F_{Sn} \sin \theta_S \right) \right],$$

$$N_B = \frac{1}{2} \left[(F_{Ay} + F_{Ey}) \left(\sin \theta - \frac{2d_P}{b} \right) + \sum_{S=A,E} \left(F_{Sn} \cos \theta_S - \frac{2d_C}{b} F_{Sn} \sin \theta_S \right) \right], \tag{13}$$

where $F_{Ay} = -T_A \times \sum_i q_{Ai} (de_{Ai} / dx_A)_{x_A=l_A}$ and $F_{Ey} = -T_E \times \sum_i q_{Ei} (de_{Ei} / dx_E)_{x_E=l_E}$ are the forces exerted by the strings A and E on the bridge in the y direction and we have dropped the subscript y from e_{Sij} and q_{Sij} .

Ignoring the constant forces F_{Sn} , lying along SC and due to the string tensioning, and using P_T as a reference point, the effect on the soundbox is now given, in place of Eq. (4), by

$$\begin{aligned}
 E_{IT}N_T + E_{IB}N_B &= E_{IT}(N_T + N_B) = E_{IT}(F_{Ay} + F_{Ey}) \\
 \sin \theta \text{ (symmetric modes)} \\
 E_{IT}N_T + E_{IB}N_B &= E_{IT}(N_T - N_B) = E_{IT} \frac{2d_P(F_{Ay} + F_{Ey})}{b} \\
 \text{(antisymmetric modes)} \\
 \text{or else } E_{IT}N_T + E_{IB}N_B &= c_I E_{IT}(F_{Ay} + F_{Ey}), \tag{14}
 \end{aligned}$$

where the c_I are force coefficients.

Moreover, the common displacements y_I of the two string extremes on the bridge may be correlated with the modal displacements of the two points P_T and P_B towards the box inside, $Q_I E_{IT}$ and $Q_I E_{IB}$ ($= \pm Q_I E_{IT}$ for the symmetric and antisymmetric modes). According to the vector diagrams of Fig. 5, one gets, considering that $y_{AI} = y_{EI} = y_I$,

$$\begin{aligned}
 y_I &= Q_I E_{IT} \sin \theta = Q_I E_{IT} c_I \text{ (symmetric modes),} \\
 y_I &= Q_I E_{IT} \frac{2d_P}{b} = Q_I E_{IT} c_I \text{ (antisymmetric modes),} \tag{15}
 \end{aligned}$$

whence a single displacement–force factor c_I may be used, with two different values for symmetric and antisymmetric modes, and it is also observable that the last equality of Eq. (14), multiplied by Q_I , and Eq. (15) combine in perfect accordance with the virtual work principle. Notice that the factor c_I may be corrected by a weighted mean of symmetric and antisymmetric values for each mode I as in the previous section.

Equation (7) has now to be written in the following form for the present case:

$$\frac{d^2 Q_I}{dt^2} + 2Z_I \Omega_I \frac{dQ_I}{dt} + \Omega_I^2 Q_I = E_{IT} c_I (F_{Ay} + F_{Ey}) \quad I = 1, 2, \dots \tag{16}$$

where Z_I is the soundbox damping factor for mode I .

As the string is a continuous system, we may introduce the one-dimensional Dirac distribution $\delta(x_S - x_{S^*})$ to manage any concentrated force F_{S^*} applied for $x_S = x_{S^*}$. In fact, when applying the modal separation procedure, its effect may be described by the integral $\int_0^{l_S} \delta(x_S - x_{S^*}) F_{S^*} e_{Sj}(x_S) dx_S = F_{S^*} e_{Sj}(x_{S^*})$. Hence, two vectors, $\{F_{SB} e_{Sj}(x_B)\}$ and $-\{F_{Sy} e_{Sj}(l_S)\}$, may be defined, where $x_B = x_{AB} = x_{EB}$ is the common value of the abscissae of the two string–bow contact points B_A and B_E , while F_{SB} is the bow force fraction acting on the one and the other string S , A and E .

Introducing the symmetric matrices $[e_{Sji}]$, where $e_{Sji} = \mu_s \int_0^{l_S} e_{Sj}(x_S) e_{Si}(x_S) dx_S$, the motion equations of the two string sub-systems may be written in the matrix form

$$\begin{aligned}
 [e_{Sji}] \left\{ \frac{d^2 q_{Si}}{dt^2} + 2\zeta_{Si} \omega_i \frac{dq_{Si}}{dt} + \omega_i^2 q_{Si} \right\}^T \\
 = \{F_{SB} e_{Sj}(x_B)\}^T - \{F_{Sy} e_{Sj}(l_S)\}^T \text{ for } S \\
 = A \text{ or } E \text{ and } i, j = 1, 2, 3, \dots \tag{17}
 \end{aligned}$$

The damping effects (Z_I and ζ_{Si}) are supposed quite small in Eqs. (16, 17) and approximately uncoupled among the various modes. Notice that the summations on the right side of Eq. (17) encompass all the modes and then all the unknowns q_{Si} , but this is not a problem in the Euler–Cauchy integration, which solves for the time derivatives, $v_i = dq_i/dt$ and dv_i/dt at each step. Observe also that q_{Si} must be considered in general as the sum of a variable part, $q_{Si-}(t)$, and a constant part q_{Si-} , which is the static part due to the mean bow force.

As specified before, the present analysis is just limited to the low modes ($< \sim 1500$ Hz), which may be clearly identified and characterized in the frequency response, whereas the high-frequency range presents the so-called "bridge hill", where a large overlap of bandwidths occurs and the present modal approach is hardly applicable. As the bridge's own frequencies are much above the examined frequency range, the bridge may be approximately considered rigid, whence the displacements $y_A(l_S, t)$ and $y_E(l_S, t)$ must be equal, as the common line of the y -axes of Fig. 5 contains both points, A and E :

$$\begin{aligned}
 y_A(l_S, t) &= \sum_i q_{Ai}(t) a_{Ai} \sin\left(\frac{\omega_i l_S}{v_{wA}}\right) = y_E(l_S, t) \\
 &= \sum_i q_{Ei}(t) a_{Ei} \sin\left(\frac{\omega_i l_S}{v_{wE}}\right). \tag{18}
 \end{aligned}$$

Here, the most significant terms of the summations are those for which $\omega_i \cong \Omega_I$, whereas the other eigenfunctions cancel out approximately for $x_S = l_S$.

If $e_{Si}(l_S) \cong 0$, that is $\omega_i l_S / v_{wS} \cong i\pi$ where i is an integer, the eigenfunctions may be in practice normalized in the usual way, assuming $a_{Si}^2 = [m_s (\int_0^1 \sin^2(i\pi x_S / l_S) d(x_S / l_S))]^{-1} = 2/m_s$, where the string mass m_s is different for each string. Otherwise, for $e_{Si}(l_S) \neq 0$, the string eigenfunctions e_{Si} cannot be normalized as usual but can be conveniently scaled all the same, to the benefit of the following calculations, so that $m_s (\int_0^1 a_{Si}^2 \sin^2(\omega_i x_S / v_{wS}) d(x_S / l_S)) = 1$, whence

$$a_{Si} = \sqrt{\frac{2}{m_s \left[1 - \left(\frac{v_{wS}}{2\omega_i l_S} \right) \sin\left(\frac{2\omega_i l_S}{v_{wS}}\right) \right]}}. \tag{19}$$

Notice that the physical dimensions of the a_{Si} are $\text{kg}^{-1/2}$, whereas those of the q_{Si} are $\text{m} \times \text{kg}^{1/2}$.

Observe that, overall, Eqs. (17) and (16) refer in practice to the same modes, i. e. the common modes of the whole coupled system string + soundbox, but only the modes for which ω_i is very close to Ω_i show non-negligible values of $e_{Sj}(l_S)$ at the string ends and give their significant contribution to the vectors $\{F_{Sy}e_{Sj}(l_S)\}^T$ on the right sides of Eq. (17). These modes are characterized by

$$Q_I = \frac{q_{SI}e_{SI}(l_S)}{c_I E_{IT}} \tag{20}$$

due to Eq. (15), where one may replace $y_I = q_{AI}e_{AI}(l_S) = q_{EI}e_{EI}(l_S) = q_{SI}e_{SI}(l_S)$ according to Eq. (18). Therefore, ascribing the subscript I to the string variables for these modes, it is possible to eliminate the Q 's from Eqs. (16) and (20), obtaining

$$\frac{d^2 q_{SI}}{dt^2} + 2Z_I \omega_i \frac{dq_{SI}}{dt} + \omega_i^2 q_{SI} = \frac{c_I^2 E_{IT}^2}{e_{SI}(l_S)} (F_{Ay} + F_{Ey}) \quad \text{for } S = A \text{ or } E. \tag{21}$$

The numerical solution can be carried out in practice simultaneously for all the q 's.

To isolate the non-linear force F_{SB} on the right side of Eq. (17) and manage this force according to the stick or slip conditions between the bow and the string, it is convenient to change Eq. (21) into the following form:

$$F_{Sy}e_{SI}(l_S) = \frac{F_{Sy}e_{SI}^2(l_S)}{(F_{Ay} + F_{Ey})c_I^2 E_{IT}^2} \left(\frac{d^2 q_{SI}}{dt^2} + 2Z_I \omega_i \frac{dq_{SI}}{dt} + \omega_i^2 q_{SI} \right) \tag{22}$$

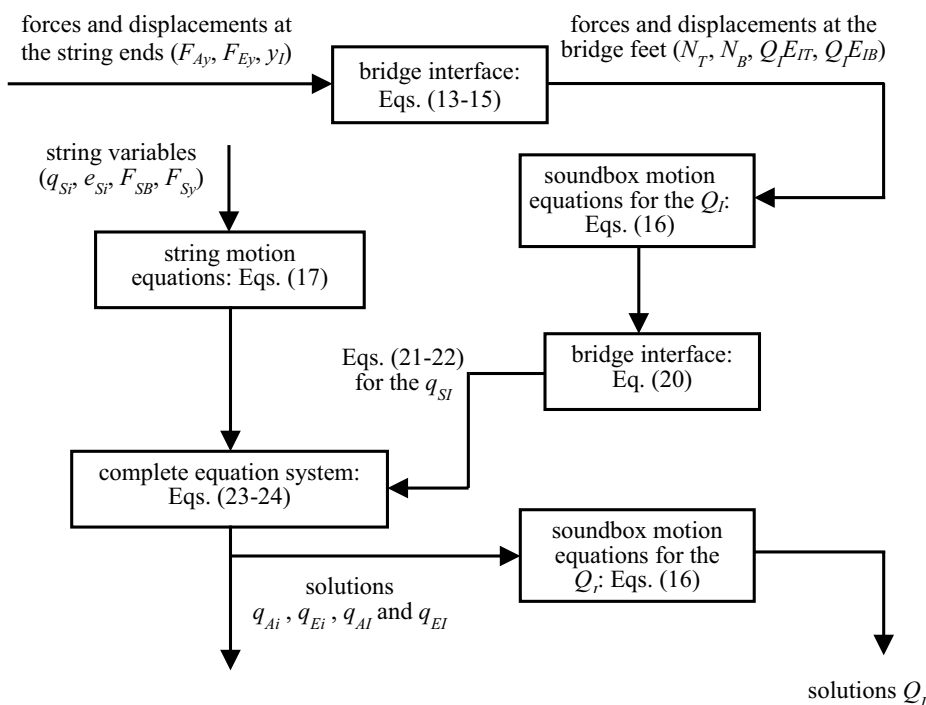
for $S = A \text{ or } E$,

replace the terms with subscripts I in the last vector on the right sides of Eq. (17) with the expression (22) and transfer these expressions to the left sides of Eq. (17). Considering that the only significant terms of the last vector on the right side of Eq. (17) are those with the subscript I , that is those for which $\omega_i \cong \Omega_i$, the mentioned transfer implies the addition of the terms on the right side of Eq. (22) to the coefficients e_{SII} of the matrix e_{Sji} , to get a new form of Eq. (17), with the only forces F_{BS} on the right sides.

Observe also that the second-order differential operators on the right side of Eq. (22) contain the damping factors Z_I of the soundbox, whereas those on the left side of Eq. (17) refer to the string damping factors ζ_{Si} . Nevertheless, the damping factors of the modes I of the strings must be considered equal to the soundbox damping factors, whence it must be here agreed that the symbols ζ_{Ai} and ζ_{Ei} assume the value Z_I for the modes I . The modified form of Eq. (17) is then

$$\begin{aligned} & \left[e_{Aji} + \frac{\delta_{ji}e_{AI}^2(l_S)F_{Ay}}{c_I^2 E_{IT}^2 (F_{Ay} + F_{Ey})} \right] \left\{ \frac{d^2 q_{Ai}}{dt^2} + 2\zeta_{Ai}\omega_i \frac{dq_{Ai}}{dt} + \omega_i^2 q_{Ai} \right\}^T \\ &= F_{BA} \{e_{Aj}(x_B)\}^T \\ & \left[e_{Eji} + \frac{\delta_{ji}e_{EI}^2(l_S)F_{Ey}}{c_I^2 E_{IT}^2 (F_{Ay} + F_{Ey})} \right] \left\{ \frac{d^2 q_{Ei}}{dt^2} + 2\zeta_{Ei}\omega_i \frac{dq_{Ei}}{dt} + \omega_i^2 q_{Ei} \right\}^T \\ &= F_{BE} \{e_{Ej}(x_B)\}^T \end{aligned} \tag{23}$$

Fig. 6 Block diagram of solution procedure for the case of two bowed strings, A4 and E5 ($S=A$ or E)



where δ_{jl} is the Kronecker delta. Hence, indicating the matrices on the left sides of Eq. (23) with $[m_{Sji}]$, for brevity, and inverting them, one obtains

$$\begin{cases} \frac{d^2 q_{Ai}}{dt^2} + 2\zeta_{Ai}\omega_i \frac{dq_{Ai}}{dt} + \omega_i^2 q_{Ai} \end{cases}^T = [m_{Aji}]^{-1} F_{BA} \{ e_{Aj}(x_B) \}^T$$

$$\begin{cases} \frac{d^2 q_{Ei}}{dt^2} + 2\zeta_{Ei}\omega_i \frac{dq_{Ei}}{dt} + \omega_i^2 q_{Ei} \end{cases}^T = [m_{Eji}]^{-1} F_{BE} \{ e_{Ej}(x_B) \}^T. \tag{24}$$

Equations (24) may be solved for the q_{Ai} and q_{Ei} and each step of the whole procedure of integration consists in solving Eq. (24) first for the q_{Si} and then Eq. (16) for the Q_j . This can be somehow considered as an "experimental" result, which tends to become all the more exact the more correct the input data are. Furthermore, it must be specified here that the direct calculation of the q_i 's by Eq. (20) gives the same results and, moreover, that the contribution of the q_i 's to the string motion results just small.

As the solution approach described so far appears somewhat complex, Fig. 6 is also introduced to gather the whole operative procedure into an explicative block diagram for a better understanding of the various steps and their concatenation.

For the string damping factors ζ_i , introducing the frequency parameters $r_i = \omega_i l_S / (\pi v_{wA})$, the following laws were used, interpolating some data from [5]:

$$2\zeta_i \omega_i \cong 5\pi(2.9 + 0.3r_i^2) \text{ s}^{-1} \text{ for } r_i \leq 3,$$

$$2\zeta_i \omega_i \cong 5\pi \frac{[5.6(10 - r_i) + 23(r_i - 3)]}{7} \text{ s}^{-1} \text{ for } r_i \geq 3. \tag{25}$$

Then, as regards the bow force F_{SB} on the string, it depends on the state of slip or stick between the string and the bow. For the former state, it is possible to assume the following function of the sliding velocity $v_{rel.} = v_B - dy_{SB}/dt$ (being v_B the bow velocity)

$$F_{SB} = F_{SB,slip} = F_s \times [0.3 + 0.7 \times \exp(-1.25 \times v_{rel.})], \tag{26}$$

where F_s is the maximum static friction force, which is a function of the normal force exerted by the violinist, who must control it in a very shrewd way. We here assume the formula $F_s = 0.05[l_S / (l_S - x_B)]^{1.5}$ N, which complies quite well with Schelleng's diagram [3].

During the stick phase, on the other hand, one has $dy_{SB}/dt = v_B = \text{constant}$, whence $d^2 y_{SB}/dt^2 = \sum_i e_{Si}(x_B) d^2 q_i / dt^2 = 0$ and, multiplying Eq. (24) by $e_{Ai}(x_B)$ and $e_{Ei}(x_B)$, respectively, and summing for all i 's, one gets

$$F_{AB} = F_{AB,stick} = \frac{\sum_i e_{Ai}(x_B) (2\zeta_{Ai}\omega_i \frac{dq_{Ai}}{dt} + \omega_i^2 q_{Ai})}{\sum_i e_{Ai}(x_B) \sum_j invm_{Aji} \times e_{Aj}(x_B)},$$

$$F_{EB} = F_{EB,stick} = \frac{\sum_i e_{Ei}(x_B) (2\zeta_{Ei}\omega_i \frac{dq_{Ei}}{dt} + \omega_i^2 q_{Ei})}{\sum_i e_{Ei}(x_B) \sum_j invm_{Eji} \times e_{Ej}(x_B)}, \tag{27}$$

where the coefficients $invm_{Sji}$ are those of the inverse matrix $[m_{Sji}]^{-1}$. The passage from the stick to the slip phase occurs automatically, during the integration, when $F_{SB,stick} = F_s$, whereas the passage from the slip to the stick phase occurs

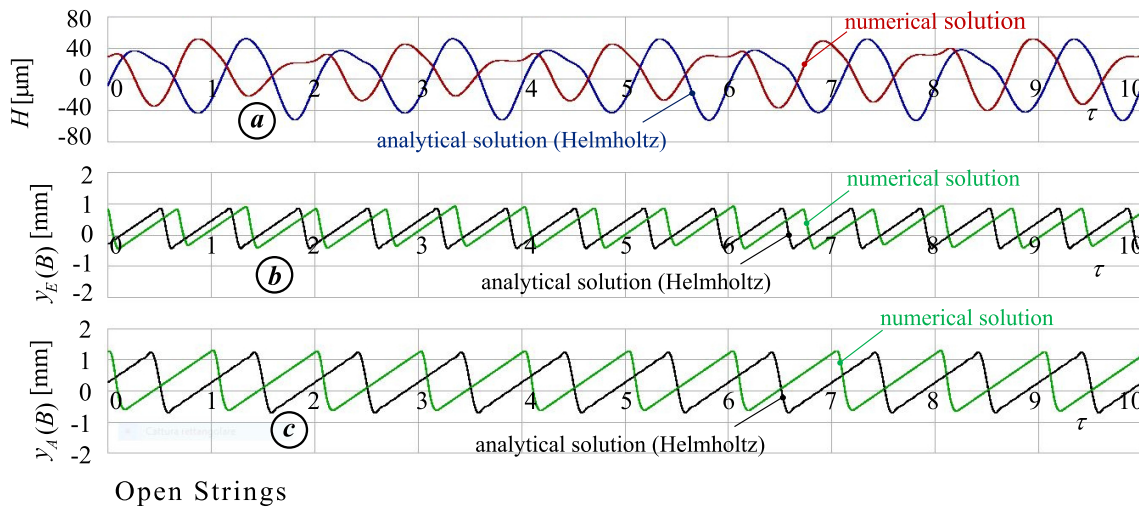


Fig. 7 String and soundbox response after a time $t_i \cong 0.25$ s, for the open string case (tones A4, E5). Time scale: $\tau = (t - t_i)v_{wA} / l_S$, $n = 10$. **a** Harmonic table vibration at reference point P_T , $H = \sum_I Q_I(t)E_{IT}$. **b** Stick–slip motion of bowed point B_E . **c** Stick–slip motion of bowed

point B_A . Data: $l_S = 325$ mm, $x_B = 285$ mm, $v_B = 1$ m/s, $T_E = 55$ N, $T_A = 45$ N, $\mu_E S_E = 0.3$ g/m, $\mu_A S_A = 0.55$ g/m. Soundbox low frequencies = 275, 400, 450, 530, 620, 850, 980 [Hz]; quality factors = 50 (all modes)

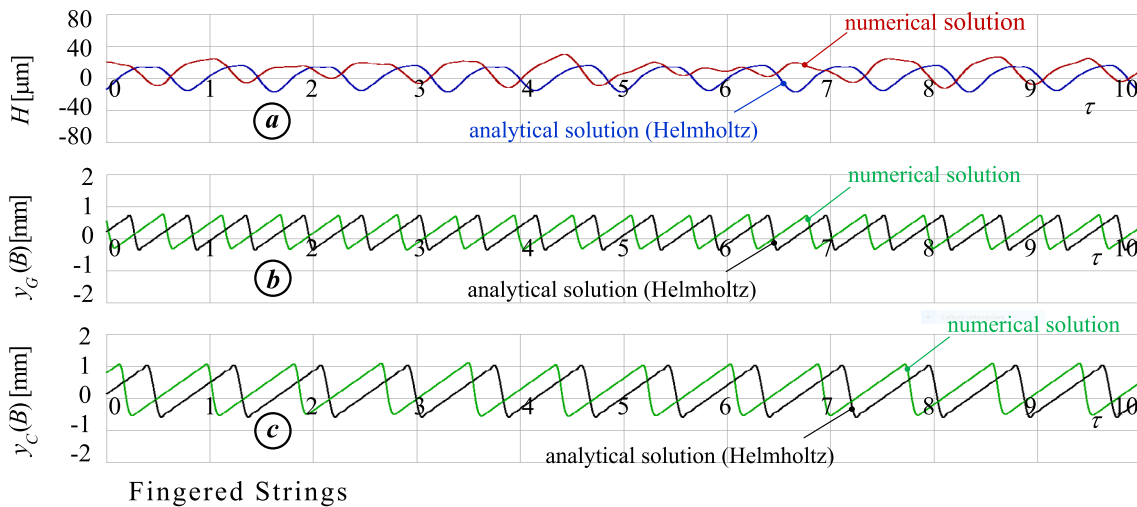


Fig. 8 String and soundbox response after a time $t_i \cong 0.25$ s, for the fingered string case (tones C5, G5). Time scale: $\tau = (t - t_i)v_{wa} / l_s$, $n = 10$. **a** Harmonic table vibration of reference point P_T , $H = \sum_l Q_l(t)E_{lT}$. **b** Stick–slip motion of bowed point B_C . **c** Stick–

slip motion of bowed point B_C . Data: $l_s = 273$ mm, $x_B = 239$ mm, $v_B = 1$ m/s, $T_G = 55$ N, $T_C = 45$ N, $\mu_G S_G = 0.3$ g/m, $\mu_C S_C = 0.55$ g/m. Soundbox low frequencies = 275, 400, 450, 530, 620, 850, 980 [Hz]; quality factors = 50 (all modes)

when $v_{rel} = 0$. Moreover, as the mean temporal bow force F_{Sm} is found to be roughly equal to the constant slip force $F_{SB,slip}$, one has $q_{Si} \cong F_{SB,slip} \sum_j [invm_{Sji} \times e_{Sj}(x_B)] / \omega_i^2$ by Eq. (24).

In parallel to the numerical solutions, analytical approximations for the soundbox motion can be also tried out expressing the $q_{Si}(t)$ by proper plausible functions, for example, assuming the Helmholtz motion for the strings, using the terms of its saw-tooth Fourier expansion,

$$q_{Si}(t) = \frac{v_B \sqrt{2m_S}}{\pi \omega_i^2} \times \frac{l_S}{(l_S - x_B)} \times \sin i\omega t \quad [m \times \sqrt{kg}] \quad (28)$$

adding the static terms q_{Si} , replacing these quantities into the right sides of the motion equations of the soundbox, Eq. (16), and solving for the $Q_{I\sim}(t)$ and $Q_{L\sim}$.

Figure 7a–c shows the time responses of the displacements: (a) of the reference point P_T of the soundbox; (b) of the bowed point B_E ; (c) of the bowed point B_A . They appear in top-down order after the steady solutions have roughly been attained (0.25 s roughly). The diagrams refer to the numerical and analytical solutions for the open chord case (A4, E5). The latter solutions are strictly periodic, while the former are nearly periodic and denote that the coupling does not distort the saw-tooth shape of the Helmholtz motion so much, which must be ascribed to the much smaller amplitude of the soundbox oscillations in comparison with the strings. Moreover, the soundbox vibrations, which are represented with a considerably smaller scale, show alternating peaks, lower and higher, to be ascribed to the different fundamental frequencies of the two vibrating chords, whose

ratio is nearly 3:2. Actually, it is easy to verify that the plots of Fig. 7a indicate with a very good approximation a period that is twice that of the fundamental harmonic of the string A4 (440 Hz) and three times that of the string E5 (659 Hz), i. e. a frequency of 220 Hz. For example, plotting aside a function of the type $y(t) = a \sin(\omega t) + b \sin(1.5\omega t + \varphi)$, one obtains diagrams quite similar to those of Fig. 7a by choosing $b/a \cong 1/2$ and $\varphi \cong 0$. This periodicity is practically exact for the analytical plots but only approximate for the numerical ones.

It must be stressed that the numerical solutions are not rigorously periodic, due to the mutual interaction between strings and soundbox, whose separated natural frequencies are not at all commensurable. Actually, the numerical responses show a small aperiodic oscillation of the amplitude and a slight shift of the phases.

It is interesting that, on varying the geometrical and mechanical characteristics of the instrument, some typical aspects of its behaviour can be detected and compared with other results present in the literature and obtained by different approaches, e.g. of the digital wave-guide kind [12]. For example, by reducing the bow force and moving the playing point under the Schelleng suggested region [3], the number of the string slip phases per period increases, revealing the occurrence of "surface sound". In practice, the results of the present approach and those of the other ones are quite similar.

Figure 8a–c refers to the case where the two strings of Fig. 7 are both fingered at the same shorter length, A4 → C5 (524 Hz), E5 → G5 (784 Hz). The results are similar to Fig. 7, but with a smaller amplitude of the soundbox

oscillations, due to increased distances of the string fundamental frequencies from the soundbox's frequencies. Also, the difference between numerical and analytical solutions appears a little more accentuated. The new playing conditions now lead to an apparent periodicity near 262 Hz ($= 524/2$ Hz) because the ratio of the fundamental frequencies of the two fingered strings is still 3:2.

Conclusion

The present report describes the vibratory behaviour of the bowed string instruments in the low-frequency range, solving the complex problem of the coupled string–soundbox vibrations numerically and trying out simple analytical approximations. The characteristic equation of the coupled system is formulated and the frequency spectrum is derived, finding the important result that the whole spectrum is nearly the union of the separated spectra of the strings and the soundbox, which is mainly due to the very smallness of the string-to-soundbox mass ratio. The time response to the bow excitation is obtained numerically by considering rigid the bridge motion and assuming a proper model of the stick–slip contact between the bow and the string. Analytical approximations to the forced motion are also calculated assuming the conventional saw-tooth shape for the string deflection, according to the Helmholtz model. The approximate solutions turn out to be periodic and sufficiently coherent with the more accurate numerical results, which are, however, non-periodic and show some very slow phase shifts and small fluctuations of amplitude compared with the analytical ones. The whole frequency spectra of the various individual instruments are certainly different from each other, as all luthiers are well aware, and, in particular, careful experimental tests should be carried out to characterize their tone colour. Yet, the present methodology may provide a useful tool to analyse the influence of possible structural or material changes of the soundbox parts on the global performances of the instruments in the low-frequency range.

The analysis may be enriched, though at the cost of increasing the complexity of the numerical calculations, by adding secondary effects, associated for example with the torsional and flexural stiffness of the strings, with the finite width of the bow–string contact, with possible changes of the speed, direction and force of the bow while playing the instrument and many other effects. An important future research line scheduled by the author regards the expansion of the analysis to the whole audible frequency range. This will demand considering also the deformability and

the vibration of the bridge and redefining its behaviour in terms of force and displacement transfer between strings and harmonic box.

Data availability The dataset supporting analysis and results is available from the author under reasonable request.

References

1. Von Helmholtz H (1912) On the sensations of tone (transl by A. J. Ellis). Longmans Green and Co., London
2. Raman CV (1918) On the mechanical theory of vibrations of bowed strings and of musical instruments of the violin family, with experimental verification of the results. *Bull Indian Assoc Cultiv Sci* 15:1–158
3. Schelleng JC (1973) Bowed string and player. *J Acoust Soc Am* 53:26–41
4. Hutchins CM (1983) A history of violin research. *J Acoust Soc Am* 53:1421–1440
5. Jansson E (2002) Acoustic for violin and guitar makers. Kung Tekniska Högskolan, Stockholm
6. Rossing TD, Fletcher NH (2004) Principles of vibration and sound. Springer
7. McIntyre ME, Woodhouse J (1979) On the fundamentals of bowed-string dynamics. *Acustica* 43(2):93–108
8. McIntyre ME, Woodhouse J (1986) Friction and the bowed strings. *Wear* 113:175–182
9. Smith JH, Woodhouse J (2000) The tribology of rosin. *J Mech Phys Solids* 48:1633–1681
10. Schumaker RT, Garoff F, Woodhouse J (2005) Probing the physics of slip-stick friction using a bowed string. *J Adhes* 81:723–750
11. Guettler K (2011) How does rosin affect sound? *String Res J* II:37–47
12. Woodhouse J (2014) The acoustic of a violin: a review, reports on progress in physics 77. IOP Publishing, Bristol, pp 1–41
13. Gough CE (2016) Violin acoustics. *Acoust Today* 12(2):22–30
14. Bissinger G (2003) Modal analysis of a violin octet. *J Acoust Soc Am* 113:2105–2113
15. Gliga VG, Stanciu MD, Nastac SM, Campean M (2020) Modal analysis of violin bodies with back plates made of different wood species. *BioResources* 15(4):7687–7713
16. Zhang A, Woodhouse J, Stoppani G (2016) Motion of the cello bridge. *J Acoust Soc Am* 140:2636–2644
17. Woodhouse J (2005) On the “bridge hill” of the violin. *Acta Acust Acust* 91:155–165
18. Sorge F (2022) On the vibrations of the bowed string instruments. In: 10th Conference on Wave Mechanics and Vibrations. July 4–6, 2022, Lisbon, Portugal

Publisher's Note Springer Nature remains neutral with regard to jurisdictional claims in published maps and institutional affiliations.

Springer Nature or its licensor (e.g. a society or other partner) holds exclusive rights to this article under a publishing agreement with the author(s) or other rightsholder(s); author self-archiving of the accepted manuscript version of this article is solely governed by the terms of such publishing agreement and applicable law.